Data Reflection Algorithm for Spectral Enhancement in Fourier Transform ICR and NMR Spectroscopies

ARTICLE *in* ANALYTICAL CHEMISTRY · OCTOBER 1995

Impact Factor: 5.64 · DOI: 10.1021/ac00115a008

2 AUTHORS:

Mikhail V Gorshkov
Russian Academy of Sciences
77 PUBLICATIONS **1,238** CITATIONS
SEE PROFILE

Richard Kouzes
Pacific Northwest National Laboratory
328 PUBLICATIONS **5,326** CITATIONS
SEE PROFILE

Anal. Chem. **1995**, *67*, 3412–3420

Data Reflection Algorithm for Spectral Enhancement in Fourier Transform ICR and NMR Spectroscopies

Michael V. Gorshkov* and Richard T. Kouzes

Environmental Molecular Sciences Laboratory, Pacific Northwest Laboratory, Battelle Boulevard, P.O. Box 999, Richland, Washington 99352

The use of a data reflection algorithm in which the signal acquired in real time is juxtaposed with the same signal reflected relatively to zero time axis through exact phase matching is considered. Because of the additional information provided by a knowledge of the exact initial phase of the signal, the resulting Fourier transform (FT) spectra have a higher resolution and signal-to-noise ratio. This algorithm was applied to ion cyclotron resonance and nuclear magnetic resonance time-domain signals. In both cases, the method improved the FT spectra compared with the original ones. It was found that artifacts may result from the time delay between the end of the excitation event and the beginning of the acquisition period, as well as from time-dependent excitation wave forms such as chirp excitation. Possible ways to decrease or eliminate the artifacts are considered. Comparison to other spectral enhancement techniques is made.

The most widely used numerical method for spectral enhancement is the Fourier transform (FT), which gives a frequency analysis of the time-domain response of a physical system.[1] The Fourier transform is the main technique for extracting spectral information in infrared (FT-IR) spectroscopy,[2] nuclear magnetic resonance (FT-NMR) spectroscopy,[3] and ion cyclotron resonance (FT-ICR) mass spectroscopy.[4,5] There are several new methods and algorithms that have been developed recently to improve the frequency spectra obtained via FT. These methods are based upon a pretransform, time-domain signal processing technique known as the magnitude-mode derivative method,[6,7] which leads to a resolution enhancement of FT spectra. In order to avoid a decrease in resolving power in a magnitude-mode FT spectrum, a FT convolution procedure has been proposed in which it was shown that the spectral line shape can be improved when the excitation frequency spectrum is known.[8,9] Other methods based upon the deconvolution of partially resolved spectra include a Fourier self-deconvolution method (FSD),[10,11] which was applied to photoelectron and NMR spectroscopies, and a peak sharpening procedure,[12] implemented recently for resolution enhancement of translational energy spectra (TES). The non-FT methods of obtaining spectral information from time-domain data are linear prediction, such as the autoregression (AR) method, and probablistic methods, such as the maximum entropy method (MEM), widely used in different physical applications.[1,13] The AR and MEM methods have some drawbacks in that they provide incorrect information when the noise level is high, and they require considerable computational time in comparison to fast Fourier transform (FFT) analysis. Another approach to obtaining the information captured in the imaginary part of the FT has recently been demonstrated by implementing the Hartley/Hilbert transform (HHT), which gives the resolving power of an absorption-mode FT and the signal-to-noise ratio (SNR) of a magnitude-mode FT by using Hilbert relations between absorption and dispersion spectra.[14]

We suggest here the use of a data reflection algorithm (DRA) for enhancing the results of FT analysis in FT-ICR and FT-NMR. The time-domain signal is replaced by a new one consisting of two juxtaposed parts: the original time-domain signal and the reflected time-domain signal. An analogy can be found in Michelson interferometry with its centerburst interferograms, which are the signals detected as a function of path length difference between different light beam components.[1] With this DRA method, we generate a centerburst time-domain spectrum which contains the phase information of the original time-domain signal, higher resolving power compared with the original magnitude-mode FT spectrum (equivalent to the resolving power of the original absorption-mode spectrum), and higher SNR and precision for the spectrum due to effective "data-fill".

THEORY

Data Reflection Algorithm for Real Time-Domain Signals. Most physical time-domain signals $f(t)$, as in the case of ICR or NMR spectroscopies, are causal functions in time, where we can write

$$f(t) = 0 \qquad \text{for } t < 0 \tag{1}$$

because normally we have no information about the system

(1) Marshall, A. G.; Verdun, F. R. *Fourier Transforms in NMR, Optical, and Mass Spectrometry: A User's Handbook*; Elsevier: Amsterdam, 1990; 460 pp.
(2) Bell, R. J. *Introductory Fourier Transform Spectrometry*; Academic Press: New York, 1972; 382 pp
(3) Ernst, R. R.; Anderson, W. A. *Rev. Sci. Instrum.* **1966**, *37*, 93–102.
(4) Comisarow, M. V.; Marshall, A. G. *Chem. Phys. Lett.* **1974**, *25*, 282–283.
(5) Comisarow, M. V.; Marshall, A. G. *Chem. Phys. Lett.* **1974**, *26*, 489–490.
(6) Balcou, Y. *Rapid Commun. Mass Spectrom.* **1994**, *8*, 942–944.
(7) Kim, H. S.; Marshall, A. G. *Private Commun. ICR/Ion Trap Newsl.* **1995**, *37*, 4–6.
(8) Marshall, A. G. *Chem. Phys. Lett.* **1979**, *63*, 515–518.
(9) Marshall, A. G.; Roe, D. C. *J. Chem. Phys.* **1980**, *73*, 1581–1590.
(10) McClure, W. F. *Spectrosc. World* **1991**, *3*, 28–34.
(11) Dromey, R. G.; Morrison, J. D.; Peel, J. B. *Chem. Phys. Lett.* **1973**, *23*, 30.
(12) Brenton, A. G.; Lock, C. M. *Rapid Commun. Mass Spectrom.* **1995**, *9*, 143–149.
(13) Ferrige, A. G.; Seddon, M. J.; Jarvis, S. *Rapid Commun. Mass Spectrom.* **1991**, *5*, 374–379.
(14) Williams, C. P.; Marshall, A. G. *Anal. Chem.* **1992**, *64*, 916–923.

0003-2700/95/0367-3412$9.00/0

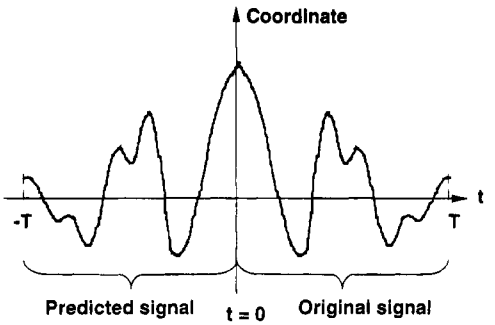

Figure 1. Schematic representation of the DRA algorithm. The resulting time domain signal has an acquisition period of $2T$, where T is the acquisition period for the originally recorded time-domain signal.

response before the detection period. The corresponding FT spectrum from such a function will reflect only the information acquired during the detection period. For example, the typical response signal in FT-ICR or FT-NMR will be an exponentially decaying cosinusoid, or the sum of cosinusoids if several different oscillators are subjected to the pulse action (excitation event):

$$f(t) = \sum_{i=1}^{N} A_i e^{-t/t_d} \cos(\omega_i t + \phi_i), \quad t \geq 0 \tag{2}$$

in which t_d is the time-decay constant determined by the rate of ion−neutral collisions in ICR spectrometry or by the spin relaxation processes in NMR spectroscopy, A_i is the corresponding ion or spin abundance, and ω_i and ϕ_i are the resonant frequencies and initial phases, respectively. In the case of ICR, the coherent spatial motion of the ions in the magnetic field is created by applying a resonant phase-coherent electric excitation field. If the energy absorbed by ions from the resonant excitation field is considerably higher than the ion initial energy (mostly thermal), the postexcitation phases ϕ_i of different ions subjected to the excitation will be the same and equal to the phase of the excitation field. Thus, for ICR or NMR spectroscopies, we can assume that we have $\phi_i = 0$ for all i in eq 2. Because $\phi_i = 0$ at $t = 0$, we may then data-fill the real time-domain signal $f(t)$ by reflection of the recorded data relative to time zero to obtain

$$f_{Inv}(t) = f(t) \qquad \text{when } t \geq 0 \tag{3}$$

$$f_{Inv}(t) = f(-t) \qquad \text{when } t < 0 \tag{4}$$

where $f_{Inv}(t)$ defines a new time-domain signal consisting of the original and reflected time-domain signals, as seen in Figure 1. In terms of a computational problem, this signal prediction is trivial and does not require time-consuming computations as in the AR or MEM algorithms. Note that the reflected discrete signal $f_{Inv}(j)$ contains $2n - 1$ data points, where n is the total number of data points in the original signal, since the data point corresponding to $t = 0$ is common for both the direct and reflected parts of the inverse array. Thus, the DRA procedure leads to the definition of the new time-domain signal $f_{Inv}(t)$ that has the acquisition period T_{Inv} elongated by a factor of 2 compared with that for the original time-domain signal. Since an improvement in resolution and SNR is not obvious for this new signal (for example, the time-decay constant remained the same), we now consider its frequency spectrum analytically.

FT Spectrum of Reflected Time-Domain Signal. The original time-domain signal $f(t)$ may be represented as the product of three well-known functions:

a cosinusoid $$s(t) = A\cos(\omega_0 t) \tag{5}$$

a boxcar $$\Pi(t/T - {}^1/_2) = 1 \qquad \text{for } 0 < t < T$$

$$\Pi(t/T - {}^1/_2) = 0 \qquad \text{for } T < t < 0 \tag{6}$$

an exponential $$e(t) = \exp(-\alpha t) \qquad \text{for } t > 0$$

$$e(t) = 0 \qquad \text{for } t < 0 \tag{7}$$

in which T is the acquisition period of the original signal, α is the decay constant, and ω_0 and A are the frequency and the amplitude of the signal, respectively.

The reflected time-domain signal $f_{Inv}(t)$ may be represented in the same way by the following functions:

a cosinusoid $$s_{Inv}(t) = A\cos(\omega_0 t) \tag{8}$$

a boxcar $$\Pi_{Inv}(t/T_{Inv} - {}^1/_2) = 1 \qquad \text{for } 0 < t < T_{Inv}$$

$$\Pi_{Inv}(t/T_{Inv} - {}^1/_2) = 0 \qquad \text{for } T_{Inv} < t < 0 \tag{9}$$

an exponential $$e_{Inv}(t) = \exp(-\alpha(t - T_{Inv}/2)) \qquad \text{for } t \geq T_{Inv}/2$$

$$e_{Inv}(t) = \exp(\alpha(t - T_{Inv}/2)) \qquad \text{for } t < T_{Inv}/2 \tag{10}$$

in which T_{Inv} is the acquisition period of the new function, $T_{Inv} = 2T$.

In accordance with the convolution theorem, we may represent the FT spectra $F(\omega)$ and $F_{Inv}(\omega)$ for the functions $f(t)$ and $f_{Inv}(t)$, respectively, as the convolution of the corresponding frequency spectra: $S(\omega)$ and $S_{Inv}(\omega)$ for cosinusoids, $\Pi(\omega)$ and $\Pi_{Inv}(\omega)$ for boxcar functions, and $E(\omega)$ and $E_{Inv}(\omega)$ for exponential functions:

$$F(\omega) = S(\omega)*\Pi(\omega)*E(\omega) \tag{11}$$

$$F_{Inv}(\omega) = S_{Inv}(\omega)*\Pi_{Inv}(\omega)*E_{Inv}(\omega) \tag{12}$$

From eqs 5–10, $S(\omega)$ and $S_{Inv}(\omega)$ give δ functions reflecting the resonant frequency, $S(\omega) = S_{Inv}(\omega) = {}^1/_2 A\delta(\omega - \omega_0)$; $\Pi(\omega)$ and $\Pi_{Inv}(\omega)$ lead to the well known sinc functions; and finally, $E(\omega)$ and $E_{Inv}(\omega)$ are responsible for the spectral peak shape. $E(\omega)$ and $E_{Inv}(\omega)$ are complex functions that can be found from the Fourier integral:

$$E(\omega) = \int_{-\infty}^{+\infty} e(t)e^{-i\omega t}\,dt = \frac{1}{\alpha(1 + \omega^2/\alpha^2)} + i\frac{\omega}{\alpha^2(1 + \omega^2/\alpha^2)} \tag{13}$$

$$E_{Inv}(\omega) = \int_{-\infty}^{+\infty} e_{Inv}(t)e^{-i\omega t}\,dt = \frac{2\cos(\omega T)}{\alpha(1 + \omega^2/\alpha^2)} + i\frac{2\sin(\omega T)}{\alpha(1 + \omega^2/\alpha^2)} \tag{14}$$

Figure 2 shows the functions $E(\omega)$ and $E_{Inv}(\omega)$ in magnitude mode. We see that the peak width of the $E_{Inv}(\omega)$ function is

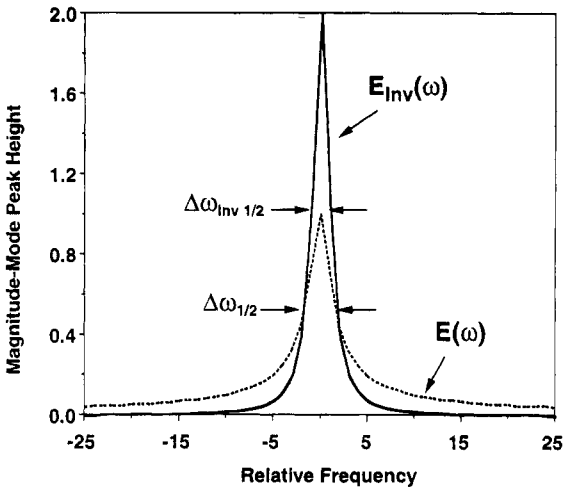

Figure 2. Comparison of the peak shape in the FT spectrum obtained for the original time-domain signal, $E(\omega)$, with that in the FT spectrum of the time-domain signal obtained via the DRA method, $E_{Inv}(\omega)$. The $E_{Inv}(\omega)$ spectrum has a higher magnitude-mode amplitude, narrower peak width, and faster peak height decay as the frequency increases.

narrower. Indeed, from eqs 13 and 14, we may find analytically

$$\Delta\omega_{1/2} = 2\sqrt{3}\alpha$$

for the magnitude-mode $E(\omega)$ function (15)

$$\Delta\omega_{Inv1/2} = 2\alpha$$

for the magnitude-mode $E_{Inv}(\omega)$ function (16)

Signal-to-Noise Ratio. By considering the magnitude-mode spectrum for the exponential functions in both cases of the original and the reflected time-domain signals, we can find from eqs 13 and 14

$$E_{magnitude}(\omega) = 1/\sqrt{\alpha^2 + \omega^2} \quad (17)$$

$$E_{Inv,magnitude}(\omega) = 2\alpha/(\alpha^2 + \omega^2) \quad (18)$$

The peak height in both cases corresponds to $\omega = 0$ and is doubled for the function $E_{Inv,magnitude}(\omega)$. This leads to the conclusion that the spectral amplitude of the reflected time-domain signal will be doubled since $S(\omega)$ and $\Pi(\omega)$ have the same magnitude-mode amplitude as $S_{Inv}(\omega)$ and $\Pi_{Inv}(\omega)$, respectively.

It is more difficult to evaluate the noise level. Since the data reflection procedure is equivalent in the DRA method to acquiring the reflected signal for twice as many counts as the original time-domain signal, the noise level will be a factor $2^{1/2}$ higher in both cases of detector-limited and source-limited noise. Thus, the resulting SNR will be increased by a factor $2^{1/2}$ in the DRA method. A separate consideration is the case of periodic noise in the original signal. The level of such noise will be increased by a factor of 2 only if its phase correlates with the phase of the signal.

Note in Figure 2 that the peak shapes are also different for the original spectrum and the spectrum obtained by the DRA method. The function $E_{Inv}(\omega)$ is not a magnitude-mode Lorentzian increased by a factor of 2, and it decays faster for frequencies far away from the resonance. Indeed, from eqs 17 and 18, we have

$$E_{Inv}(\omega)/E(\omega) = 2/\sqrt{1 + (\omega/\alpha)^2} \to 0 \qquad \text{when } \omega \to \infty \quad (19)$$

This fact is important since this gives an additional improvement in the peak separation of spectra obtained via the DRA method.

RESULTS AND DISCUSSION

FT-ICR Applications. Figure 3a shows a simulated time-domain signal and FT spectrum for a mass doublet of equal ion abundance. The DRA signal and the corresponding FT spectrum are shown in Figure 3b. In this calculation, we simulated Gaussian random noise at the level of 20% of the level of the acquired signal. The use of the DRA method improves considerably not only the resolution and SNR but also the accuracy in determining the relative peak intensities as a result of better peak separation. In Figure 4a, we show a doublet with frequencies so close to each other that the peaks in the FT spectrum cannot be resolved. By applying the data reflection algorithm, peak separation becomes possible (Figure 4b). This example directly shows that the proposed DRA procedure leads to additional information in FT spectra as well as better looking spectra.

The data reflection algorithm has been applied to actual experimental FT-ICR data. In Figure 5a, the mass spectrum from bovine insulin is shown. The ions were formed in the electrospray source (ESI) of a 7-T FT-ICR spectrometer at Pacific Northwest Laboratory.[16] The spectrum corresponds to the $[M + 4H]^{4+}$ protonated multiply-charged molecular ion with a characteristic isotopic peak pattern. The acquired time-domain signal was 2 MB in size. The DRA mass spectrum is shown in Figure 5b.

Use of the Data Reflection Algorithm for Quadrature Detection. The method of data reflection for acquired time-domain signals may be used for real and complex data, such as for the case of quadrature detection that is typically used in NMR spectroscopy and can also be applied to ICR.[1] In quadrature detection, the signal from the excited spins (or ions) is acquired from two detection channels applied to the system's degrees of freedom, which are 90° out of phase with each other.[15] The resulting time-domain signal is the complex array with both nonzero real and imaginary parts. Both parts make a contribution to the FT spectrum.

Figure 6a shows the simulated time-domain data and the corresponding FT spectrum typical in NMR spectroscopy with quadrature detection. In Figure 6b, the same data were transformed by applying the DRA procedure. Note that for the imaginary part of the time domain, the time reversed part is also 180° phase inverted to provide correct juxtaposition between the original data and the predicted data. The resulting reflected time domain, which has real and imaginary parts, was subjected to the complex FT in the same way as the original data. We see that the applied algorithm improved the resolution and SNR in accordance with eqs 15 and 16.

The data reflection processing of a quadrature detected signal has been applied to an experimental ^{111}Cd solid sample in NMR.

(15) Fukushima, E.; Roeder, S. B. W. *Experimental Pulse NMR: A Nuts and Bolts Approach*; Addison-Wesley Publishing Co., Inc., Advances Book Program: Reading, PA, 1981; 539 pp.

(16) Winger, B. E.; Hofstadler, S. A.; Bruce, J. E.; Udseth, H. R.; Smith, R. D. *J. Am. Soc. Mass Spectrom.* **1993**, *4*, 566–577.

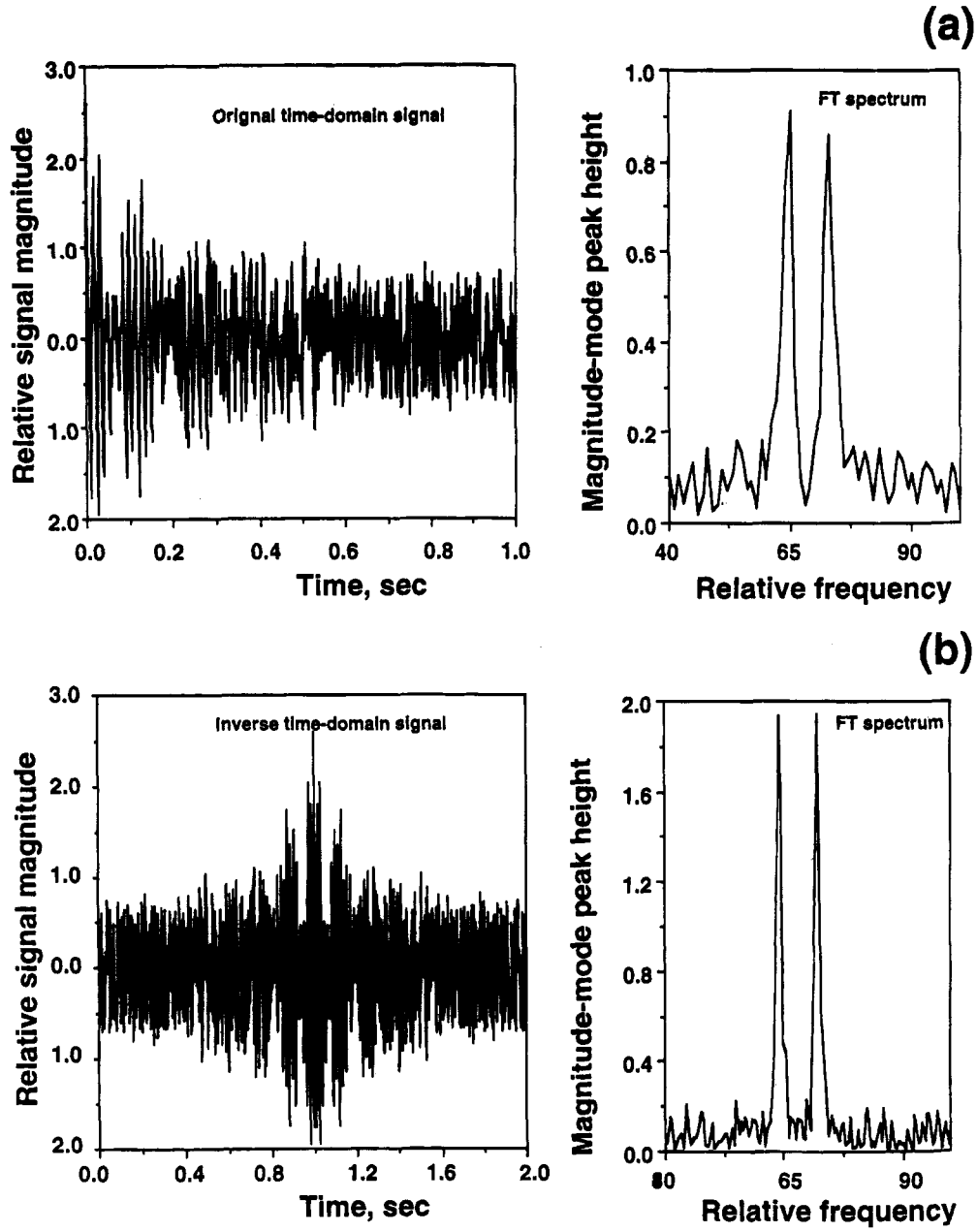

Figure 3. (a) Simulated time-domain signal (left) and the corresponding FT spectrum (right) for a mass doublet with equal peak abundance. (b) Time-domain signal obtained via the DRA method and the corresponding FT spectrum for the same mass doublet.

Data were obtained in the quadrature detection mode on a 300-MHz NMR spectrometer. The real and imaginary parts of the time-domain signal had 512 data points. The ^{111}Cd NMR spectrum contains more than 10 characteristic peaks, which can be recognized in Figure 7a. The reflected time-domain signal and the corresponding FT spectrum are shown in Figure 7b. The improvement in resolution and SNR is obvious, although artifacts appear in the spectrum. The main reason for artifacts in this particular case was associated with the presence of postexcitation relaxation of the receiver when the signal was acquired. To eliminate this postexcitation relaxation, two data points have been dropped from the beginning of the original time-domain signal. This procedure thus perturbed the phase matching between the direct time and the predicted parts. Additionally, the quadrature detection method is sensitive to the phase difference between the real and imaginary parts of the time domain signal.

Below, we consider in more details the artifacts associated with the proposed DRA method and the ways to eliminate them.

Artifacts. There will be no artifacts when all oscillators in the system under study are excited simultaneously, as in the case of single frequency excitation. This is also true when the harmonics in the excitation wave form, which correspond to the oscillators of different eigenfrequencies, have the same phases. In these cases, all excited oscillators (ions or spins) will have the same phases at the end of the excitation event, and phase matching in the DRA procedure may be done correctly. In practice, there is a time delay between excitation and detection. Thus, if there are several oscillators of different frequencies but the same phases when the excitation event is ended, the delay before detection leads to different phases at the moment the detection is started. This is not crucial for magnitude-mode FT spectra, which are not sensitive to the initial phase (Figure 8). But for the data reflection procedure, the initial phase is crucial to the correct juxtaposition of the original and predicted time-domain signals. Any delay leads to incorrect phase matching between the original and predicted parts, as is shown in Figure

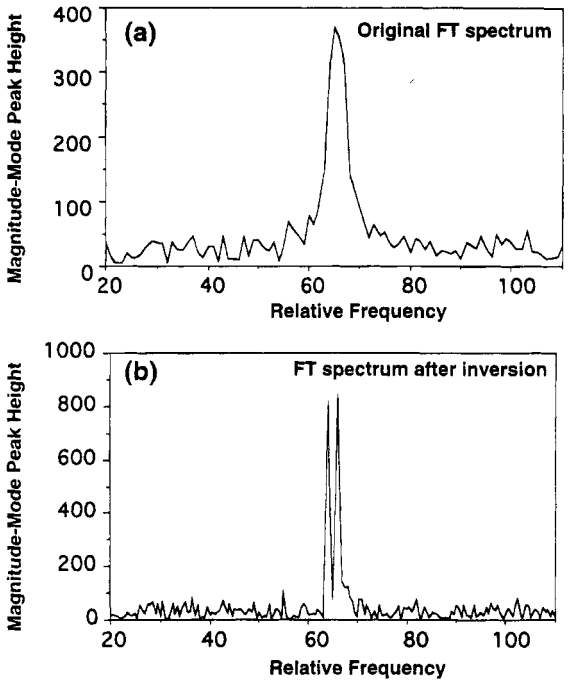

Figure 4. (a) FT spectrum of an unresolved mass doublet with equal peak abundance. (b) FT spectrum for the same doublet after the DRA method was applied to the original time-domain signal.

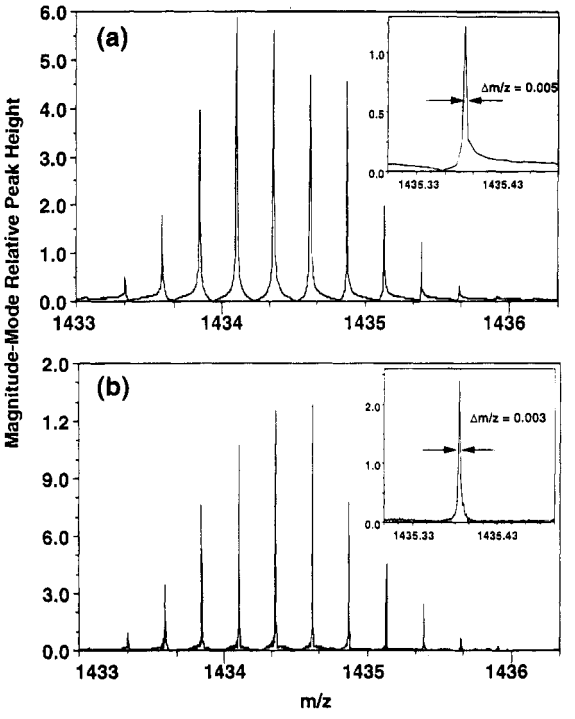

Figure 5. (a) $[M + 4H]^{4+}$ molecular ion mass spectrum of bovine insulin obtained in magnitude-mode FT by using an electrospray ion source interfaced with a 7-T FT-ICR mass spectrometer.[16] The average mass resolution for the peaks was 250 000 defined as $m/\Delta m_{50\%}$, where $\Delta m_{50\%}$ is the full peak width at half-maximum peak height (fwhm). (b) FT magnitude-mode mass spectrum for the same ions after the DRA method was applied to the original time-domain signal. The average mass resolution (fwhm) for the peaks was 450 000.

9a for the same data as in Figure 8. The expanded view of the time-domain signal shows the phase mismatch at the central data point. This results in loss of information about the system. One of the possible ways to avoid this problem is to find the nearest maximum in the original time-domain signal. This maximum corresponds to the point of phase synchronization for all oscillators in accordance with the principle of superposition for harmonic oscillations and with the assumption of synchronized oscillations at the moment the excitation ended (in practice, this becomes complex for multiple ion situations, as discussed later). For instance, for a doublet with two eigenfrequencies, ω_1 and ω_2, the maxima in the time-domain signal correspond to the following times τ_{max} after the excitation:

$$\tau_{max} = 2\pi n/(\omega_1 - \omega_2), \quad n = 0, 1, 2, \ldots \tag{20}$$

In most practical cases, the time interval between nearest maxima is small, and this suggested method of time shifting is equivalent to a slight elongation of the delay. Figure 9b shows the data reflected signal and corresponding FT spectrum for the same doublet as Figures 8 and 9a, for which the phase matching was corrected in the above-described way.

This method for eliminating artifacts by time shifting is not effective if (1) the number of oscillators is too large or (2) the oscillators have been excited by broadband chirp excitation. In these cases, a more general method of artifact elimination can be suggested: phase correction in the complex FT spectrum of the original time-domain data. Since all of the experimental parameters for the excitation and the delays before detection are known, a phase correction procedure can be performed in all practical cases. Consider the original time-domain signal consisting of N harmonic oscillators:

$$f(t) = \sum_{i=0}^{N-1} A_i \cos(\omega_i t - \phi_i) \tag{21}$$

where ϕ_i represents the individual phases that have to be corrected. This means that the phase of the ith peak has to be rotated by ϕ_i. The corresponding FT spectrum will be defined by the following expression:

$$F(\omega) = \sum_{-\infty}^{+\infty} f(t)\, e^{-i\omega t}\, dt = \sum_{i=0}^{N-1} F_i(\omega) \tag{22}$$

in which $F_i(\omega)$ is the complex frequency spectrum corresponding to the individual oscillator,

$$F_i(\omega) = \int_{-\infty}^{+\infty} A_i \cos(\omega_i t - \phi_i)\, e^{-i\omega t}\, dt$$
$$= \mathrm{Re}_i(\omega) + i\mathrm{Im}_i(\omega) \tag{23}$$

where $\mathrm{Re}_i(\omega)$ and $\mathrm{Im}_i(\omega)$ are the real and imaginary parts of the Fourier spectrum, respectively. Each phase may then be corrected by obtaining the pure absorption $\mathrm{Ab}_i(\omega)$ and dispersion $\mathrm{De}_i(\omega)$ spectra that correspond to $\phi_i = 0$. This may be done by the procedure of phase rotation described elsewhere:[1]

$$\mathrm{Ab}_i(\omega) = \mathrm{Re}_i(\omega) \cos \phi_i - \mathrm{Im}_i(\omega) \sin \phi_i \tag{24}$$

$$\mathrm{De}_i(\omega) = \mathrm{Re}_i(\omega) \sin \phi_i + \mathrm{Im}_i(\omega) \cos \phi_i$$

The resulting corrected FT spectrum $F_c(\omega)$ will be

$$F_c(\omega) = \sum_{i=0}^{N-1} \mathrm{Ab}_i(\omega) + i\mathrm{De}_i(\omega) \tag{25}$$

and the following inverse Fourier transform will give time-domain data that will correspond to the original data but synchronized in phase for all oscillators. Thus, we have

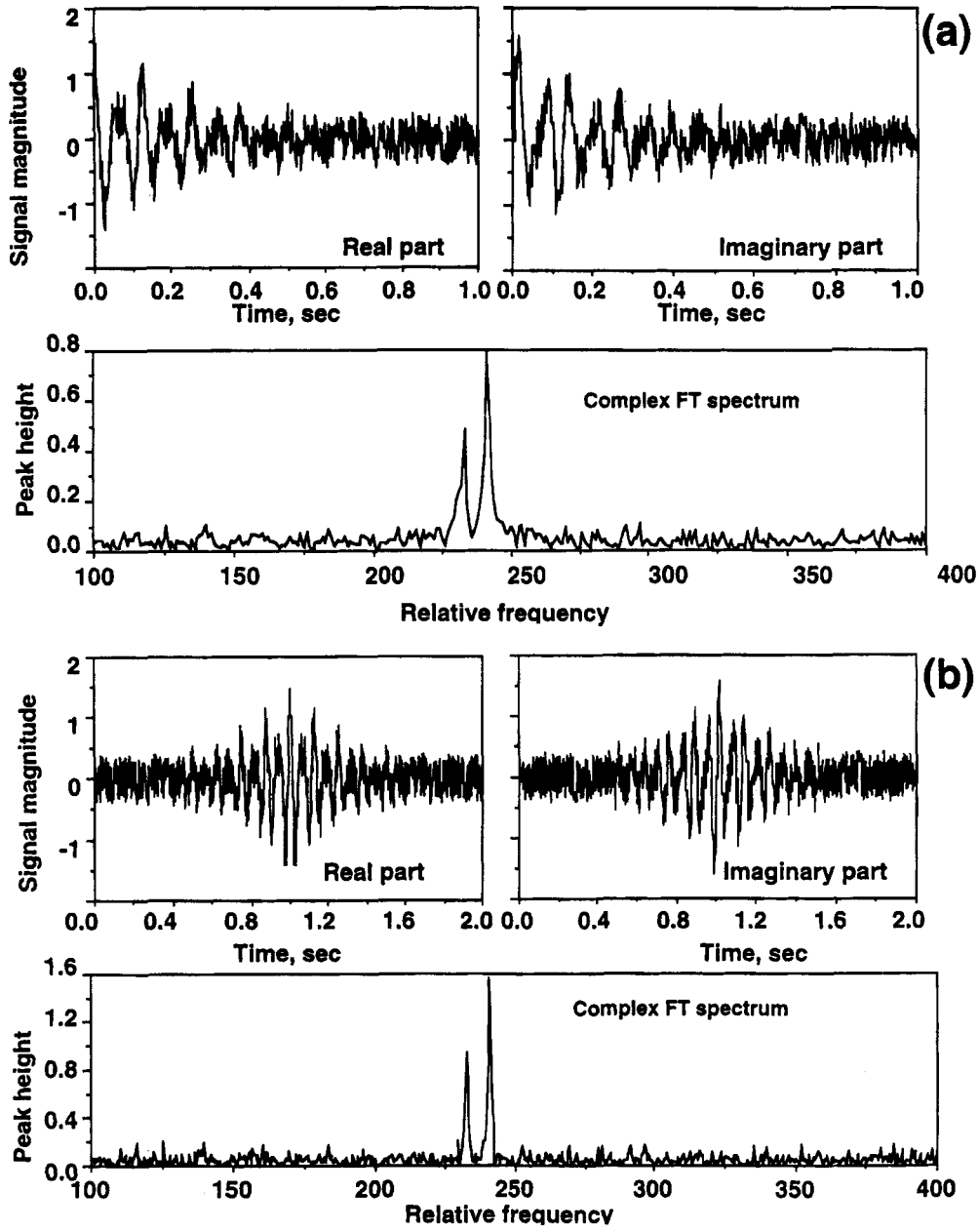

Figure 6. Use of the DRA method for time-domain data obtained by the method of quadrature detection followed by a complex Fourier transform. (a) Simulated real and imaginary parts of the original signal (top) and corresponding frequency spectrum. (b) Real and imaginary parts of the signal obtained via the DRA method from the same original data. The DRA imaginary part was created by both time and phase inversion.

$$f_c(t) = F^{-1}[F_c(\omega)] = \int_{-\infty}^{+\infty} F_c(\omega)\, e^{i\omega t}\, d\omega$$

$$= \sum_{i=0}^{N-1} \int [Ab_i(\omega) + iDe_i(\omega)]\, e^{i\omega t}\, d\omega$$

$$= \sum_{i=0}^{N-1} \int_{-\infty}^{+\infty} [Re_i(\omega) + iIm_i(\omega)] e^{i(\omega t + \phi_i)}\, d\omega$$

$$= \sum_{i=0}^{N-1} f_i(t)\, e^{i\phi_i} \qquad (26)$$

That is, the phase of each oscillator will be corrected to be the same and equal to zero.

Figure 10 shows the result of applying the phase correction procedure to a spectrum in which the oscillators were excited by chirp excitation. Each oscillator had an individual phase before correction (Figure 10a), resulting in a poor result from the data reflection procedure (Figure 10d). The phases of each oscillator were then corrected in accordance with eqs 24–26 to give a pure absorption spectrum (Figure 10b). The following inverse FT gave the time-domain signal in which the phases of all oscillators were the same and equal to zero in accordance with eq 26. The DRA procedure was then applied for spectral enhancement (Figure 10e).

Comparison of the DRA Method with Prior Work and Its Limitations. The DRA method can be compared to the method of data-filling suggested by Watson and Eyler.[18] Their method

(17) Bartholdi, E.; Ernst, R. R. *J. Magn. Reson.* **1973**, *11*, 9–19.
(18) Watson, C. H.; Eyler, J. R. Proceedings of the 36th ASMS Conference on Mass Spectrometry and Allied Topics; San Francisco, CA, June 5-10, 1988; pp 600–601.

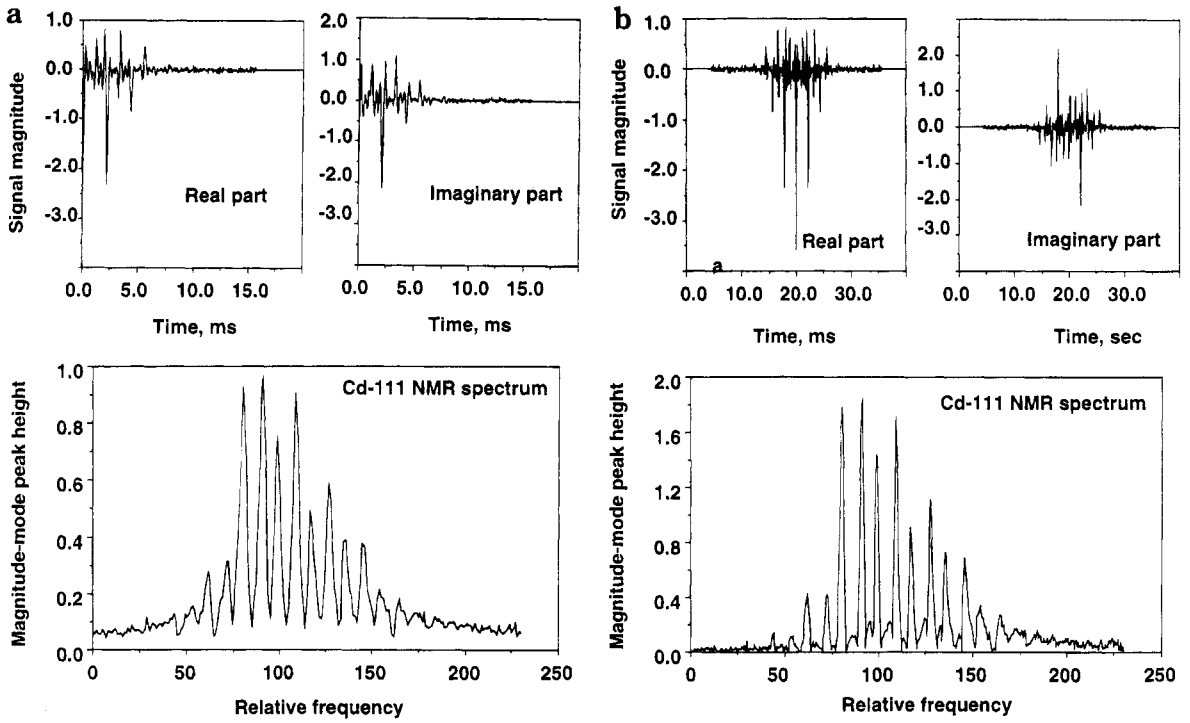

Figure 7. (a) Experimental time-domain signal and the corresponding NMR frequency spectrum of ^{111}Cd obtained by quadrature detection with a 300-MHz NMR spectrometer. (b) Time-domain signal and the corresponding NMR frequency spectrum obtained after application of the DRA method.

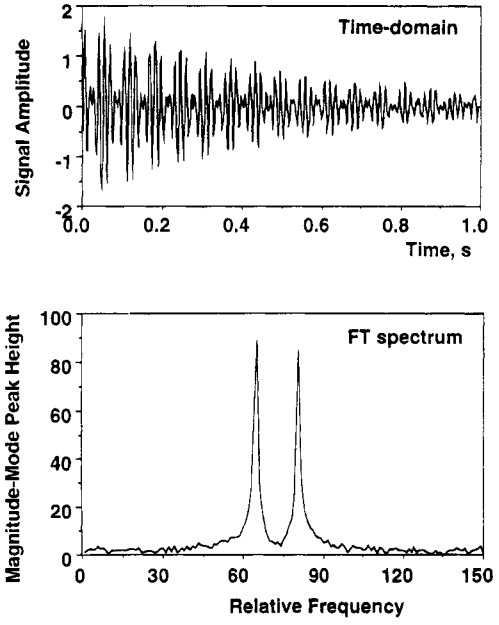

Figure 8. Simulated time-domain signal (top) and the corresponding FT spectrum (bottom) of the mass doublet for equal ion abundance. A 10-ms delay between the end of excitation and the beginning of detection was applied, which does not effect the frequency spectrum in magnitude mode.

was based upon time-domain signal elongation by juxtaposing the original data set with the same data set starting at the end of the acquisition period. This method has the major limitation of losing the phase information when the SNR is decreasing at the end of acquisition period. In the work described herein, we use data-filling through an algorithm of data reflection about zero time where the phase information is fixed by the predetection history and the SNR is high.

Another approach to the problem of recovering the information stored in the imaginary part of an FFT is to use time-domain zero-filling as proposed by Bartholdi and Ernst and widely used in practice to transfer some of the information residing in the disperion-mode FT into the absorption mode.[17] Because the time domain is elongated by zeroes, not all the information is taken back into the magnitude-mode FT. The resolution improvement is not as great as in the DRA method, and the SNR does not change. Figure 11 shows a comparison between the magnitude-mode FT from a simulated FT-ICR signal obtained by a regular FFT without zero-filling, a regular FT with a single pretransform zero-fill, and the DRA method without zero-filling. Obviously, the zero-fill procedure improves the peak shape and the precision of peak measurements because of a larger number of data points. The DRA method adds spectral enhancement because it contains both phase restoration and data-filling. Moreover, the DRA method gives a better resolving power for a magnitude-mode FT spectrum compared with that of an absorption-mode FT.

An alternative method for spectral enhancement is the Hartley/Hilbert transform algorithm proposed by Williams and Marshall recently, in which the information residing in the dispersion-mode FT spectrum is recovered by using Hilbert relations between absorption and dispersion FT.[14] This method gives an enhanced absorption spectrum which has the resolution of the absorption mode FT, which is better than that of the magnitude-mode FT by a factor of $3^{1/2}$, and the SNR of the magnitude-mode FT, which is better than that of the absorption-mode FT by a factor of $2^{1/2}$. In the DRA method, the same improvement in resolving power is achieved, together with a SNR increased by a factor of $2^{1/2}$ compared with the magnitude-mode FT and hence by a factor of 2 compared with the absorption-mode FT. Note that the DRA algorithm requires twice the number of data points to be processed as in the HHT method, but this is compensated by the trivial programming procedure for data reflection.

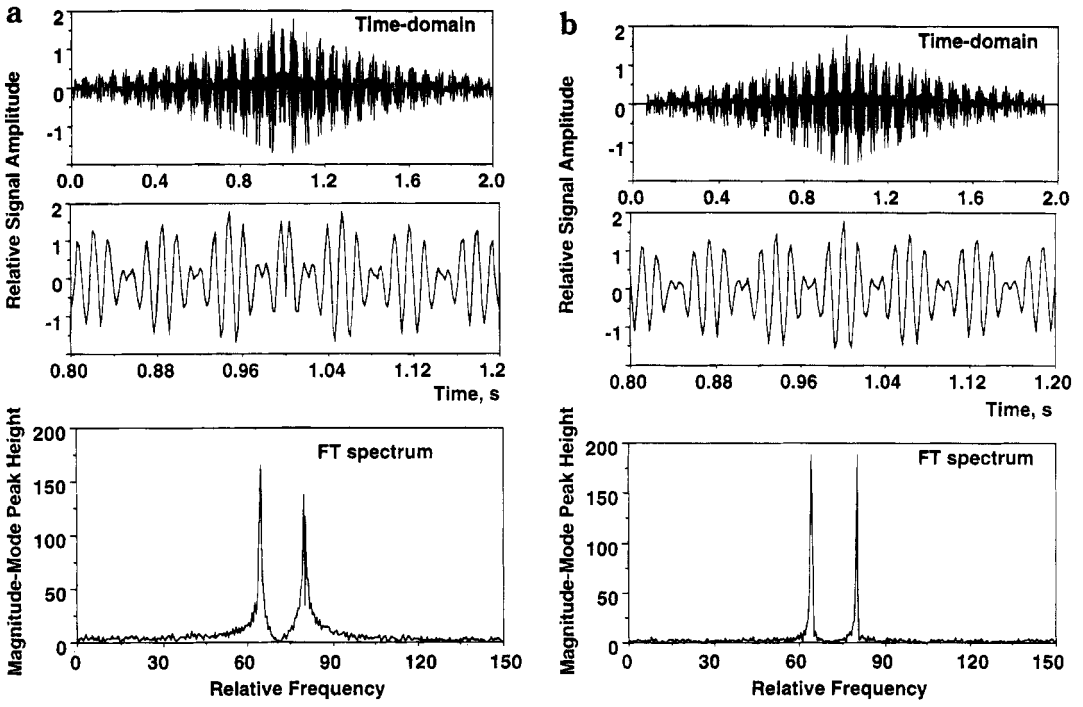

Figure 9. (a) Time-domain signal (top) and the corresponding FT spectrum (bottom) obtained via the DRA method for the same doublet as in Figure 8. The phase mismatch is shown in the extended figure (middle). The resulting FT spectrum is distorted and shows no improvement in resolution or signal-to-noise ratio. (b) The same signal after phase correction for both oscillators by choosing the first maximum in the beat pattern of the original time-domain signal shown in Figure 8. The DRA procedure leads to spectral enhancement compared with the original data.

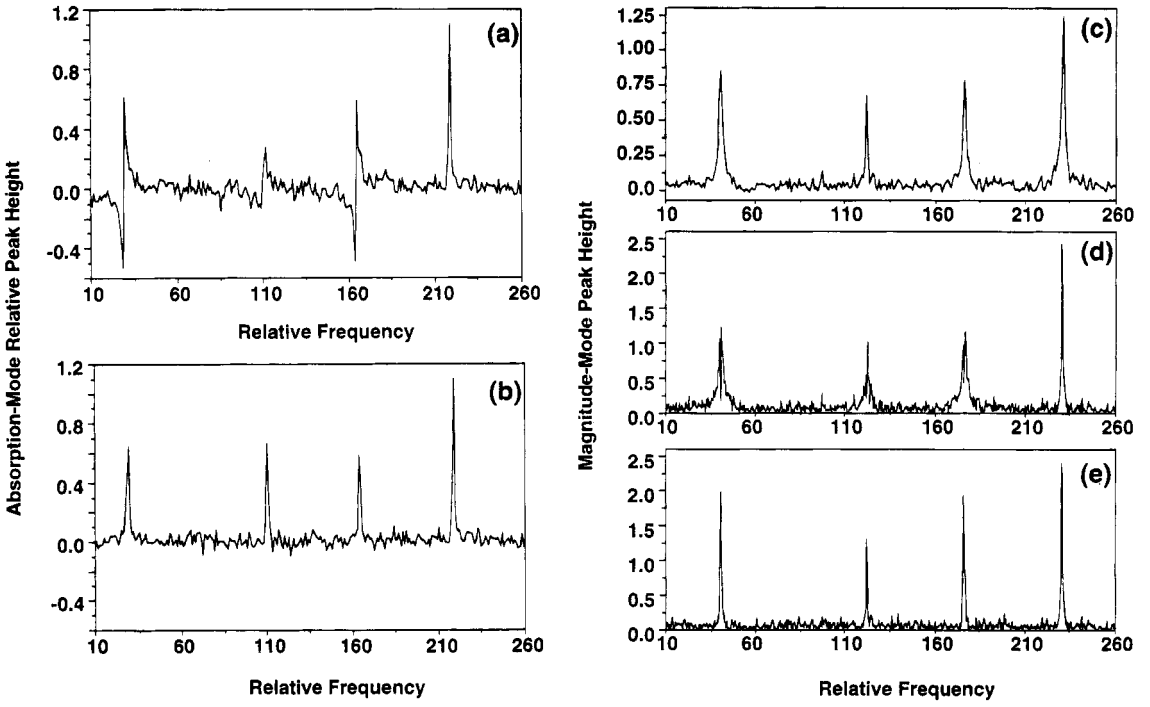

Figure 10. (a) Real part of a simulated FT spectrum for a multioscillator system. The oscillators were excited by chirp excitation, in which the excitation frequency was scanned over the frequency range of these oscillators. As a result, when detection is started, each of the oscillators has an individual phase. (b) Real part of the FT spectrum for the same system of oscillators after phase correction. The phases of all oscillators were corrected to be zero at the moment the detection is started. (c) FT magnitude-mode spectrum obtained for the original time-domain signal. (d) FT magnitude-mode spectrum obtained for the DRA transformed time domain signal corresponding to the data in (a) before the phase correction is applied. (e) FT magnitude-mode spectrum obtained for the DRA transformed time domain signal corresponding to the data in (b) after the phase correction is applied.

Both the DRA and HHT algorithms are limited in the case of frequency sweep excitation proposed by Comisarow and Marshall in FT-ICR[5] by the neccesity of having the phases of all oscillators the same at time zero. The phase of the system response depends nonlinearly on the frequency. One of the possible solutions is a deconvolution technique proposed by Marshall for use in FT-ICR-MS.[8,9] In this method, the response of each oscillator $h(t)$ to a δ function excitation is recovered from the frequency spectrum of

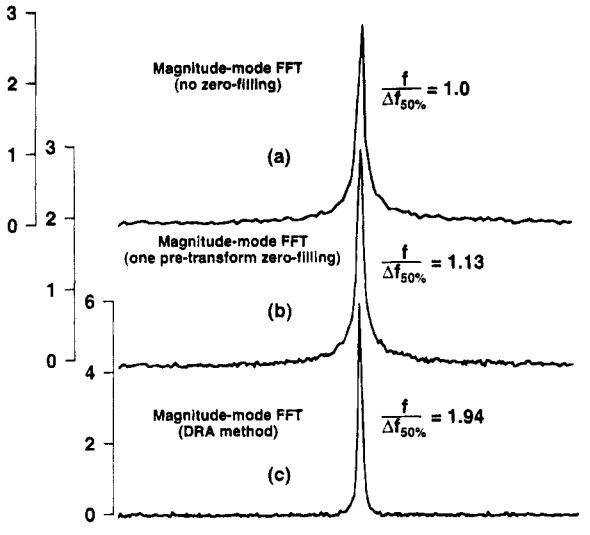

Figure 11. Comparison of the magnitude-mode FT spectrum (a) with those obtained by using a single zero-filling procedure (b) and by using a data reflection algorithm (c). The frequency resolution (fwhm) obtained by using the DRA method is higher by a factor of $3^{1/2}$ compared with that of a single zero-filled spectrum for the same number of data points in both spectra.

the excitation wave form Exc(ω) and the frequency spectrum of the detected signal $F(\omega)$,

$$F(\omega) = \mathrm{Exc}(\omega)\cdot H(\omega) \qquad (27)$$

followed by the inverse FT. This technique is limited to the case of a short delay between excitation and detection. In particular, the deconvolution technique is simple when detection occurs simultaneously with excitation or when there is no delay between excitation and detection.[9]

CONCLUSIONS

The results presented have shown that the simple procedure of juxtaposing the original time-domain signals obtained in FT-ICR spectrometry and FT-NMR spectroscopy with the same data set reversed in time improves the resolution of the corresponding FT spectra by a factor of $3^{1/2}$ and the SNR by a factor of $2^{1/2}$ compared with the magnitude-mode FFT and by a factor 2 compared with absorption-mode FFT. The procedure is equivalent to predicting the signal that the system of harmonic oscillators had when time was negative. The phase matching between the original and predicted parts of the signal obtained after inversion is the key aspect of getting additional information from the spectrum. The advantage of the proposed DRA procedure, compared with other existing methods of signal prediction or improving the spectral data, is the simplicity of the algorithm, which does not require time-consuming computational operations. Another advantage of the DRA method is the improvement of both the resolution and the SNR.

It was found that in some practical cases, when the oscillators under study are not excited simultaneously, as in the case of broadband chirp excitation, artifacts in the FT spectrum appeared. These artifacts may be eliminated by appropriate correction of the phases of each individual oscillator in the frequency spectrum of the original time-domain signal in combination with the inverse Fourier transform.

The data reflection algorithm may be especially helpful in quick analysis of poorly resolved or unresolved spectra in FT-ICR-MS and FT-NMR spectroscopy, as well as for the identification of unknown low-intensity peaks in noisy spectra because of the higher resolving power and SNR in DRA spectra.

ACKNOWLEDGMENT

This research was supported by Associated Western Universities under Grant DE-FG06-89ER-75522 with the U.S. Department of Energy and by The Laboratory Directed Research and Development Program at Pacific Northwest Laboratory (PNL). PNL is a multiprogram national laboratory operated by Battelle Memorial Institute for the U.S. Department of Energy under Contract DE-AC06-76RLO 1830. We thank Gordon A. Anderson, Herman M. Cho, and Andy S. Lipton for providing experimental FT-ICR and FT-NMR data. We also thank Alan G. Marshall, Shenheng Guan, and Michael W. Senko from The National High Magnetic Field Laboratory for useful discussions on the subject of this paper.

Received for review March 13, 1995. Accepted June 20, 1995.[⊗]

AC9502561

[⊗] Abstract published in *Advance ACS Abstracts*, August 1, 1995.